

RESEARCH MEMORANDUM

INVESTIGATION OF THE LONGITUDINAL

AERODYNAMIC CHARACTERISTICS OF A TRAPEZOIDAL-WING

AIRPLANE MODEL WITH VARIOUS VERTICAL POSITIONS OF

WING AND HORIZONTAL TAIL AT MACH

NUMBERS OF 1.41 AND 2.01

By Gerald V. Foster

Langley Aeronautical Laboratory Langley Field, Va.

NATIONAL ADVISORY COMMITTEE FOR AERONAUTICS

WASHINGTON

March 6, 1958 Declassified October 28, 1960

NATIONAL ADVISORY COMMITTEE FOR AERONAUTICS

RESEARCH MEMORANDUM

INVESTIGATION OF THE LONGITUDINAL

AERODYNAMIC CHARACTERISTICS OF A TRAPEZOIDAL-WING

AIRPLANE MODEL WITH VARIOUS VERTICAL POSITIONS OF

WING AND HORIZONTAL TAIL AT MACH

NUMBERS OF 1.41 AND 2.01

By Gerald V. Foster

SUMMARY

An investigation has been conducted in the Langley 4- by 4-foot supersonic pressure tunnel to determine the effects of various vertical positions of a wing and horizontal tail on the static longitudinal aerodynamic characteristics of a trapezoidal-wing airplane model at Mach numbers of 1.41 and 2.01. The model was equipped with a wing and horizontal tail having 0° sweep of the 75-percent-chord line. The wing had an aspect ratio of 3, taper ratio of 0.25, and 4-percent-thick circularare airfoil sections. The unswept horizontal tail had an aspect ratio of 4, taper ratio of 0.60, and 4-percent-thick hexagonal airfoil sections. The model was also tested with a 45° sweptback horizontal tail with an NACA 65A006 airfoil section and aspect ratio and taper ratio identical with the unswept tail.

In general, the effects of wing vertical position at Mach numbers 1.41 and 2.01 are similar to those obtained at subsonic speeds. Experimental lift and pitching-moment characteristics of the midwing tail-off configuration indicated a slightly lower lift-curve slope for Mach number 1.41 and a less negative pitching-moment-curve slope for both Mach numbers than predicted by theory. For the tail-on configuration, experimental and predicted lift characteristics agreed fairly well; however, experimental pitching-moment characteristics indicated a 5-percentgreater static margin at Mach number 1.41 and a 4-percent-lower static margin at Mach number 2.01 than predicted. A change in vertical position of the unswept horizontal tail from low to high resulted in a positive trim change with and without the wing. Incorporating 450 sweepback in the horizontal tail on the midwing configuration at a Mach number of 1.41 decreased the positive trim change of the high-tail configuration but had no appreciable effect on the longitudinal characteristics of the low-tail configuration.

INTRODUCTION

A knowledge of the effects of wing and horizontal-tail position on the aerodynamic characteristics of wing-body configurations is important in the aerodynamic design of an aircraft. Experimental studies have yielded a considerable amount of such information at subsonic speeds (for example, see refs. 1 to 4); however, at the present only limited amounts of such information are available in the supersonic speed range (for example, see refs. 5 to 7).

Recently, a study at Mach numbers of 1.41 and 2.01 has been conducted in the Langley 4- by 4-foot supersonic pressure tunnel to provide additional information concerning the effects at supersonic speeds of wing and horizontal-tail vertical position and horizontal-tail plan form on the aerodynamic characteristics of a model having trapezoidal lifting surfaces. The longitudinal phase of the investigation is presented herein.

SYMBOLS

The results are presented as coefficients of forces and moments and are referred to the stability-axis system with the reference center of moments located at 25 percent of the wing mean geometric chord.

The symbols used herein are defined as follows:

wing span, ft

$c_{\mathtt{L}}$	lift coefficient, Lift/qS
C'D	drag coefficient, Drag/qS
$C_{\mathbf{m}}$	pitching-moment coefficient, Pitching moment/qSc
Δc_{m_t}	tail pitching-moment contribution, C _m tail on - C _m tail off
q	free-stream dynamic pressure, lb/sq ft
М	Mach number
S	wing area, sq ft
С	local chord, ft
ē	mean geometric chord, ft

it horizontal-tail incidence angle, deg

L/D lift-drag ratio

α angle of attack, deg

x_{cp} center of pressure, percent c

MODEL.

The geometric characteristics of the model are given in figure 1 and table I. The wing was constructed of steel and had an aspect ratio of 3.0, a taper ratio of 0.25, and 0° sweep at the 75-percent-chord line. The thickness ratio of the wing was 0.04 and the airfoil section, parallel to the plane of symmetry, is a symmetrical circular arc. The body, composed of an ogive nose, a cylindrical midsection, and a slightly boattailed afterbody, had a fineness ratio of 11. The wing was attached to the body in either a high, mid, or low position. The unswept horizontal tail had 16.6° sweepback of the quarter-chord line, an aspect ratio of 4, a taper ratio of 0.6, and 4-percent-thick hexagonal sections. An alternate horizontal tail had 45° sweepback of the quarter-chord line and NACA 65A006 airfoil section. The horizontal tail was mounted on the vertical fin at vertical positions of the tail referred to as "high tail" and "low tail" located 0.382b/2 above and 0.208b/2 below the body center line, respectively. Provisions were made for manually varying the incidence angle of the horizontal tail from 0° to -6°.

TESTS, CORRECTIONS, AND ACCURACY

Force and moment measurements were made through the use of a six-component internal strain-gage balance attached to a rotary-type sting. The conditions of the tests were as follows:

Mach number 1.41	2.01
Stagnation pressure, lb/sq in. abs 10) 10
Stagnation temperature, OF 100	100
Reynolds number based on \bar{c} 2.23 \times 10 ⁶	1.84 × 10 ⁶

The stagnation dewpoint was maintained sufficiently low (-25° F or less) so that no significant condensation effects were encountered in the test section.

The sting angle was corrected for the deflection under load. The base pressure was measured and the drag force was adjusted to a base pressure equal to the free-stream static pressure.

The estimated errors in the individual measured quantities are as follows:

	M = 1.41	M = 2.01
C_{L}	±0.0056	±0.0069
C _D	±0.0005	±0.0006
C _m	±0.0022	±0.0027
i ₊ , deg	±0.2	±0.2
α, deg	0.2	0.2

The Mach number variation in the test section was approximately ± 0.1 and the flow-angle variation in the vertical and horizontal plane did not exceed about $\pm 0.1^{\circ}$.

RESULTS AND DISCUSSION

Effect of Wing Vertical Position

The longitudinal aerodynamic characteristics of wing-body configurations presented in figures 2 to 4 show the effects of wing vertical position at M = 1.41 and M = 2.01. At a Mach number of 1.41, the effect of wing position appears to result primarily in a shift in the center of pressure (fig. 4) coupled with small changes in lift and drag (fig. 2). For example, at a constant angle of attack the high-wing configuration has a slightly lower lift and a more forward center of pressure and thus a less negative pitching moment than the midwing configuration, whereas the converse is true for the low wing. The change in lift due to wing position is associated with body induced negative pressure on the lower surface of the high wing and on the upper surface of the low wing. Both the high- and low-wing configurations had higher drag than the midwing configuration at $\alpha = 0^{\circ}$ and this amounted to an incremental drag coefficient of approximately 0.0020. At the higher Mach number (M = 2.01) (fig. 3), change in wing position had no effect on the lift or drag at low angles of attack up to approximately 80 but did tend to alter the center of pressure and thus resulted in changes in pitching moment similar to those noted for M = 1.41. In the moderate and high angle-of-attack range, the pitching moments of the high-wing and midwing configurations are essentially the same; whereas the low-wing configuration exhibited a less negative pitching moment than either the midwing or the high-wing configuration. The reason for this relative decrease in pitching moment for the low wing is not clearly understood but it would appear to be associated with the effects of wake interference of the low wing on the afterbody at moderate and high angles of attack. In general the effects of wing position at angle of attack up to approximately 8° on the longitudinal stability characteristics are similar to the effects indicated for subsonic speeds. (See ref. 1, for example.)

Theoretical predictions of the variation of lift and pitching-moment characteristics of the wing-body configuration with angle of attack were made based on the method of reference 8. This method is based on a planar model and limited to low angles of attack. The theory (figs. 2(a) and 3(a)) indicates slightly larger values of $C_{L_{\alpha}}$ at M = 1.41 and a more negative value of $C_{m_{\alpha}}$ at both Mach numbers than obtained experimentally.

The lift-drag ratio (fig. 5) for M=2.01 is not affected by change in wing position within limits of the investigation; whereas, for M=1.41 either an increase or a decrease in wing position relative to the midwing resulted in a decrease in lift-drag ratio particularly in the region of maximum lift-drag ratio.

Tail-On Characteristics

Longitudinal aerodynamic characteristics of the wing-body-tail configurations and body-tail configurations obtained at M = 1.41 and M = 2.01 are presented in figures 6 to 13. The effect of wing position for a given horizontal-tail position and the effect of horizontal-tail position for a given wing position on the longitudinal stability characteristics are shown in figures 14 and 15, respectively. The effect of the wing on the pitching-moment contribution of the unswept horizontal tail is shown in figure 16. The data presented in figures 17 and 18 show the effect of sweep of the horizontal tail. The trim characteristics for the various wing and horizontal-tail positions are given in table II.

In general, the pitching-moment characteristics obtained with a given horizontal tail (fig. 14) indicate that the wing vertical position had a relatively small effect on the longitudinal stability at M=1.41 and M=2.01. It is of interest to note, however, that at M=1.41 change from high to low wing tended to increase the static margin at moderate lift coefficients with the high-tail arrangement; whereas with the low-tail arrangement a comparable change in wing vertical position tended to decrease the static margin. A comparison of the tail

pitching-moment contribution (fig. 16) tends to indicate that these changes in static margin are probably associated with the wing interference flow field on the tail.

Theoretical predictions of the lift and pitching-moment characteristics for the wing-body-tail configuration were based on reference 8. As previously stated, this method is based on a planar model; consequently, it does not account for the effects of vertical position of the wing or tail. Interferences resulting from downwash in the region of the tail caused by the wing vortices have been included in these predictions. It may be noted in figures 7(a) and 10(a) that the experimental and estimated lift characteristics of the tail-on configuration agree fairly well; however, the experimental pitching-moment characteristics indicate a 5-percent-greater static margin at Mach number 1.41 and a 4-percent-lower static margin at Mach number 2.01 than predicted.

The most significant effect of horizontal-tail position is associated with the trim characteristics. Figure 15 indicates that a change in vertical position of the tail from low to high resulted in a positive trim change. Hence, the drag incurred with the high-tail configuration for a given trim condition might be expected to be less than with the low-tail configuration. The validity of this is beyond the limitation of the present investigation since the trim characteristics were obtained for only two tail incidence angles; however, reference 7 indicated that for a swept-wing—tail arrangement, a horizontal tail located in a vertical position comparable to that of the present high tail provided a slightly larger lift-drag ratio than a low-tail configuration at a trimmed lift coefficient of 0.20 and greater.

The primary effect at M=1.41 of increasing the sweepback of the horizontal tail from 16.6° at the quarter-chord line to 45° at the quarter-chord line (fig. 17) is to decrease the positive trim change associated with the high tail; whereas, the effects of the change in sweep of the low tail on the longitudinal stability characteristics were negligible. The variation of pitching-moment coefficient with Mach number obtained at $\alpha=0^{\circ}$ for the swept and unswept horizontal tail are presented in figure 18. The results for the swept tail and body were obtained in a previous investigation of which a portion is reported in reference 7. It may be noted that at M=1.41 the presence of the wing in the midposition does not alter the effect of tail sweep on $C_{\rm m}$ at $\alpha=0^{\circ}$.

CONCLUSIONS

An investigation of the effects of various vertical positions of a wing and horizontal tail on the static longitudinal aerodynamic characteristics of a trapezoidal-wing model at Mach numbers of 1.41 and 2.01

indicated the following conclusions:

l. The high-wing configuration had slightly lower lift and a less negative pitching moment than the midwing configuration for angles of attack up to approximately 8°, whereas the converse was true for the low wing. In general, these effects of wing vertical position are similar to those obtained at subsonic speeds.

- 2. Experimental lift and pitching-moment characteristics of the midwing tail-off configuration indicated a slightly lower lift-curve slope for Mach number 1.41 and a less negative pitching-moment-curve slope for both Mach numbers than predicted by theory. For the tail-on configuration, experimental and predicted lift characteristics agreed fairly well; however, experimental pitching-moment characteristics indicated a 5-percent-greater static margin at Mach number 1.41 and a 4-percent-lower static margin at Mach number 2.01 than predicted.
- 3. Change in vertical position of the unswept horizontal tail from low to high resulted in a positive trim change with or without the wing.
- 4. Incorporating 45° sweepback in the horizontal tail on the midwing configuration at a Mach number of 1.41 decreased the positive trim change of the high-tail configuration but had no appreciable effect on the longitudinal characteristics of the low-tail configuration.

Langley Aeronautical Laboratory,
National Advisory Committee for Aeronautics,
Langley Field, Va., December 13, 1957.

REFERENCES

- 1. Goodman, Alex: Effects of Wing Position and Horizontal-Tail Position on the Static Stability Characteristics of Models With Unswept and 45° Sweptback Surfaces With Some Reference to Mutual Interference.

 NACA TN 2504, 1951.
- 2. Queijo, M. J., and Wolhart, Walter D.: Experimental Investigation of the Effect of Vertical-Tail Size and Length and of Fuselage Shape and Length on the Static Lateral Stability Characteristics of a Model With 45° Sweptback Wing and Tail Surfaces. NACA Rep. 1049, 1951. (Supersedes NACA TN 2168.)
- 3. Morrison, William D., Jr., and Alford, William J., Jr.: Effects of Horizontal-Tail Position and a Wing Leading-Edge Modification Consisting of a Full-Span Flap and a Partial-Span Chord-Extension on the Aerodynamic Characteristics in Pitch at High Subsonic Speeds of a Model With a 45° Sweptback Wing. NACA TN 3952, 1957. (Supersedes NACA RM L53E06.)
- 4. Furlong, G. Chester, and McHugh, James G.: A Summary and Analysis of the Low-Speed Longitudinal Characteristics of Swept Wings at High Reynolds Number. NACA Rep. 1339, 1957. (Supersedes NACA RM L52D16.)
- 5. Heitmeyer, John C.: Effect of Vertical Position of the Wing on the Aerodynamic Characteristics of Three Wing-Body Combinations. NACA RM A52L15a, 1953.
- 6. Spearman, M. Leroy: Investigation of the Aerodynamic Characteristics in Pitch and Sideslip of a 45° Sweptback-Wing Airplane Model With Various Vertical Locations of the Wing and Horizontal Tail Effect of Wing Location and Geometric Dihedral for the Wing-Body Combination, M = 2.01. NACA RM L55B18, 1955.
- 7. Spearman, M. Leroy, and Driver, Cornelius: Investigation of Aerodynamic Characteristics in Pitch and Sideslip of a 45° Sweptback-Wing Airplane Model With Various Vertical Locations of Wing and Horizontal Tail - Static Longitudinal Stability and Control, M = 2.01. NACA RM L55L06, 1956.
- 8. Nielsen, Jack N., Kaattari, George E., and Anastasio, Robert F.: A Method for Calculating the Lift and Center of Pressure of Wing-Body-Tail Combinations at Subsonic, Transonic, and Supersonic Speeds. NACA RM A53GO8, 1953.

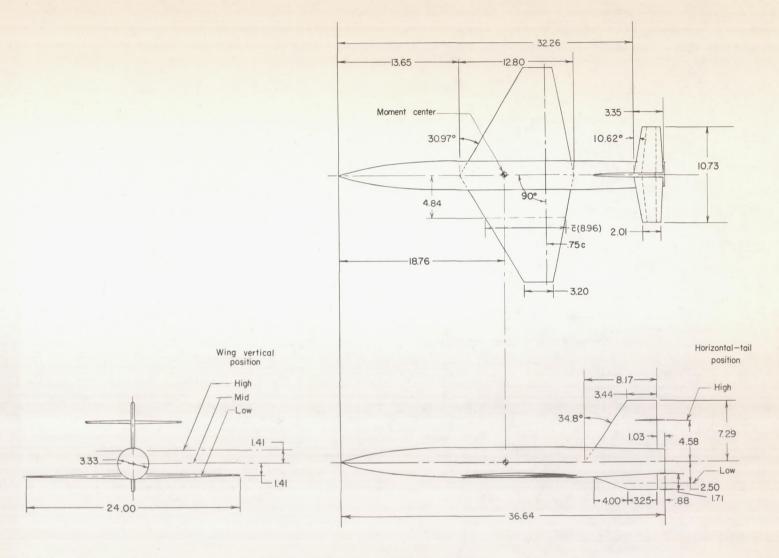
В

TABLE I.- GEOMETRIC CHARACTERISTICS OF MODEL

Wing:	
	192
Span, in	-
	.20
	.25
Aspect ratio	3
Mean geometric chord, in	.96
Spanwise location of mean geometric	. 50
chord, percent wing semispan	40
, 1	0
Sweep of 75-percent-chord line, deg	0
Airfoil section 4-percent circular-	arc
Body:	
Length, in	.64
Diameter (maximum), in	.33
Diameter (base), in	
Length-diameter ratio	
Horizontal Tail:	
Trapezoidal -	
Area, sq in	
Span, in	
Root chord, in	
Tip chord	
Taper ratio	.60
	4
Sweep of 75-percent-chord line, deg	0
	0
Sweep of 75-percent-chord line, deg	0 nal
Sweep of 75-percent-chord line, deg	onal 8.6
Sweep of 75-percent-chord line, deg	0 nal 8.6
Sweep of 75-percent-chord line, deg	0 nal 8.6 .73
Sweep of 75-percent-chord line, deg	0 nal 8.6 .73 .35
Sweep of 75-percent-chord line, deg Airfoil section 4-percent hexagor Sweptback - Area, sq in. 28 Span, in. 10 Root chord, in. 3 Tip chord, in. 22 Taper ratio 0	0 nal 8.6 •73 •35 •01
Sweep of 75-percent-chord line, deg Airfoil section 4-percent hexagor Sweptback - Area, sq in. 28 Span, in. 10 Root chord, in. 3 Tip chord, in. 2 Taper ratio 0 Aspect ratio	0 nal 8.6 •73 •35 •01 •60
Sweep of 75-percent-chord line, deg Airfoil section 4-percent hexagor Sweptback - Area, sq in. 28 Span, in. 10 Root chord, in. 3 Tip chord, in. 2 Taper ratio 0 Aspect ratio Sweep of quarter-chord line, deg	0 nal 8.6 .73 .35 .01 .60 45
Sweep of 75-percent-chord line, deg Airfoil section 4-percent hexagor Sweptback - Area, sq in. 28 Span, in. 10 Root chord, in. 3 Tip chord, in. 2 Taper ratio 0 Aspect ratio	0 nal 8.6 .73 .35 .01 .60 45
Sweep of 75-percent-chord line, deg Airfoil section 4-percent hexagon Sweptback - Area, sq in. 28 Span, in. 10 Root chord, in. 3 Tip chord, in. 2 Taper ratio 2 Aspect ratio 3 Sweep of quarter-chord line, deg Airfoil section NACA 65AC	0 nal 8.6 .73 .35 .01 .60 45
Sweep of 75-percent-chord line, deg Airfoil section 4-percent hexagon Sweptback - Area, sq in. 28 Span, in. 10 Root chord, in. 3 Tip chord, in. 2 Taper ratio 2 Aspect ratio 3 Sweep of quarter-chord line, deg Airfoil section NACA 65AC	0 nal 8.6 •73 •35 •01 •60 4 45
Sweep of 75-percent-chord line, deg Airfoil section 4-percent hexagon Sweptback - Area, sq in. 28 Span, in. 10 Root chord, in. 3 Tip chord, in. 2 Taper ratio 2 Aspect ratio 3 Sweep of quarter-chord line, deg Airfoil section NACA 65AC	0 nal 8.6 ·73 ·35 ·01 ·60 ·45 006
Sweep of 75-percent-chord line, deg Airfoil section 4-percent hexagon Sweptback - Area, sq in. 28 Span, in. 10 Root chord, in. 3 Tip chord, in. 2 Taper ratio 2 Aspect ratio 3 Sweep of quarter-chord line, deg Airfoil section NACA 65AC	0 nal 8.6 ·73 ·35 ·01 ·60 ·45 006 3.5 ·29
Sweep of 75-percent-chord line, deg Airfoil section 4-percent hexagon Sweptback - Area, sq in. 28 Span, in. 10 Root chord, in. 2 Tip chord, in. 2 Taper ratio 2 Aspect ratio 3 Sweep of quarter-chord line, deg Airfoil section NACA 65AC	0 nal 8.6 ·73 ·35 ·01 ·60 ·45 006 3.5 ·29 ·17
Sweep of 75-percent-chord line, deg Airfoil section 4-percent hexagon Sweptback - Area, sq in. 28 Span, in. 10 Root chord, in. 3 Tip chord, in. 2 Taper ratio 0 Aspect ratio 5 Sweep of quarter-chord line, deg Airfoil section NACA 65AC Vertical tail: Area to body center line, sq in. 4 Span from body center line, in. 7 Root chord, in. 8 Tip chord, in. 3	0 nal 8.6 · 73 · 35 · 01 · 60 · 4 · 45 · 60 · 60 · 3 · 5 · 29 · 17 · 44
Sweep of 75-percent-chord line, deg Airfoil section 4-percent hexagon Sweptback - Area, sq in. 26 Span, in. 10 Root chord, in. 3 Tip chord, in. 2 Taper ratio 0 Aspect ratio Sweep of quarter-chord line, deg Airfoil section NACA 65A0 Vertical tail: Area to body center line, sq in. 4 Span from body center line, in. 7 Root chord, in. 8 Tip chord, in. 8 Tip chord, in. 3 Taper ratio 0	0 nal 8.6 · 73 · 35 · 01 · 60 · 4 · 45 006 3 · 5 · 29 · 17 · 44 · 42
Sweep of 75-percent-chord line, deg Airfoil section 4-percent hexagor Sweptback - Area, sq in. 26 Span, in. 10 Root chord, in. 3 Tip chord, in. 2 Taper ratio 0 Aspect ratio Sweep of quarter-chord line, deg Airfoil section NACA 65AC Vertical tail: Area to body center line, sq in. 45 Span from body center line, in. 7 Root chord, in. 8 Tip chord, in. 8 Tip chord, in. 3 Taper ratio 0 Aspect ratio 0 Aspect ratio 1	0 nal 8.6 ·73 ·35 ·01 ·60 ·45 ·006 ·3 ·5 ·29 ·17 ·44 ·42 ·29
Sweep of 75-percent-chord line, deg Airfoil section 4-percent hexagor Sweptback - Area, sq in. 26 Span, in. 10 Root chord, in. 3 Tip chord, in. 22 Taper ratio 0 Aspect ratio 0 Sweep of quarter-chord line, deg Airfoil section NACA 65AC Vertical tail: Area to body center line, sq in. 45 Span from body center line, in. 7 Root chord, in. 8 Tip chord, in. 8 Tip chord, in. 8 Taper ratio 0 Aspect ratio 0 Aspect ratio 1 Sweep of leading edge, deg	0 nal 8.6 ·73 ·35 ·01 ·60 ·45 ·006 ·3 ·5 ·29 ·17 ·44 ·42 ·29 ·35
Sweep of 75-percent-chord line, deg Airfoil section	0 nal 8.66 · 73 · 35 · 01 · 60 · 45 · 006 · 59 · 17 · 44 · 42 · 29 35 · 0n -
Sweep of 75-percent-chord line, deg Airfoil section 4-percent hexagor Sweptback - Area, sq in. 26 Span, in. 10 Root chord, in. 3 Tip chord, in. 22 Taper ratio 0 Aspect ratio 0 Sweep of quarter-chord line, deg Airfoil section NACA 65AC Vertical tail: Area to body center line, sq in. 45 Span from body center line, in. 7 Root chord, in. 8 Tip chord, in. 8 Tip chord, in. 8 Taper ratio 0 Aspect ratio 0 Aspect ratio 1 Sweep of leading edge, deg	0 nal 8.66 · 73 · 35 · 01 · 60 · 45 · 006 · 59 · 17 · 44 · 42 · 29 35 · 0n -
Sweep of 75-percent-chord line, deg Airfoil section 4-percent hexagor Sweptback - Area, sq in. 26 Span, in. 10 Root chord, in. 3 Tip chord, in. 2 Taper ratio 0 Aspect ratio 0 Sweep of quarter-chord line, deg Airfoil section NACA 65AC Vertical tail: Area to body center line, sq in. 45 Span from body center line, in. 7 Root chord, in. 3 Tip chord, in. 3 Taper ratio 0 Aspect ratio 1 Sweep of leading edge, deg Airfoil section Negge nose, slab side with constant thickness of 0.437 in	0 nal 8.66 · 73 · 35 · 01 · 60 · 45 · 006 · 59 · 17 · 44 · 42 · 29 35 · 0n -
Sweep of 75-percent-chord line, deg Airfoil section	0 nal 8.6 · 73 · 35 · .01 · .60 4 45 6 006 5 · 29 · .17 · .44 2 · .29 35 · .00 ch

TABLE II.- SUMMARY OF TRIM CHARACTERISTICS

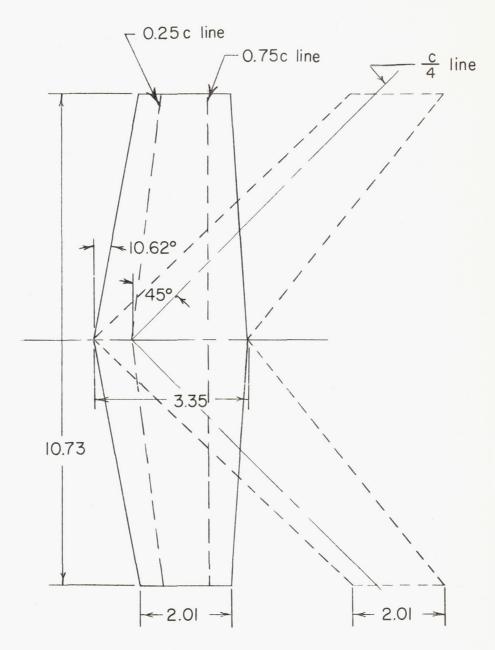
Configuration		α, deg	$\mathtt{c}_{\mathtt{L}}$	c^{D}	L/D	α, deg	$c_{ m L}$	$C^{\mathbb{D}}$	L/D
Wing	Unswept horizontal tail		i _t =	= 0 ⁰			it	= - 6°	
M = 1.41									
High High Mid Mid Low Low	High Low High Low High Low	2.5 1.1 2.1 .7 1.9	0.125 .050 .110 .037 .110	0.0410 .0365 .0370 .0340 .0380	3.05 1.37 2.96 1.06 2.90	7.1 4.8 6.3 4.9 5.9 5.2	0.367 .250 .337 .269 .310	0.0855 .0582 .0735 .0590 .0895 .0620	4.28 4.28 4.57 4.56 3.46 4.55
M = 2.01									
High High Mid Mid Low Low	High Low High Low High Low	1.9 .2 2.6 .5 3.5	0.070 .020 .100 .020 .130	0.0340 .0340 .0360 .0340 .0360	2.06 .60 2.78 .60 3.60	5.9 3.5 6.1 3.9 7.9 4.3	0.215 .130 .236 .150 .290 .160	0.0500 .0380 .0520 .0390 .0720 .0480	4.30 3.42 4.42 3.84 4.00 3.33



(a) Details of complete model.

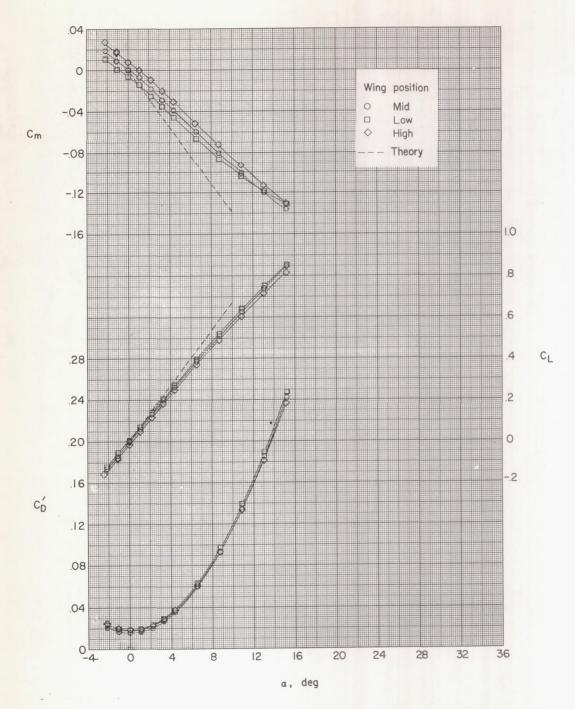
Figure 1.- Geometry of complete model. All dimensions in inches except as noted.





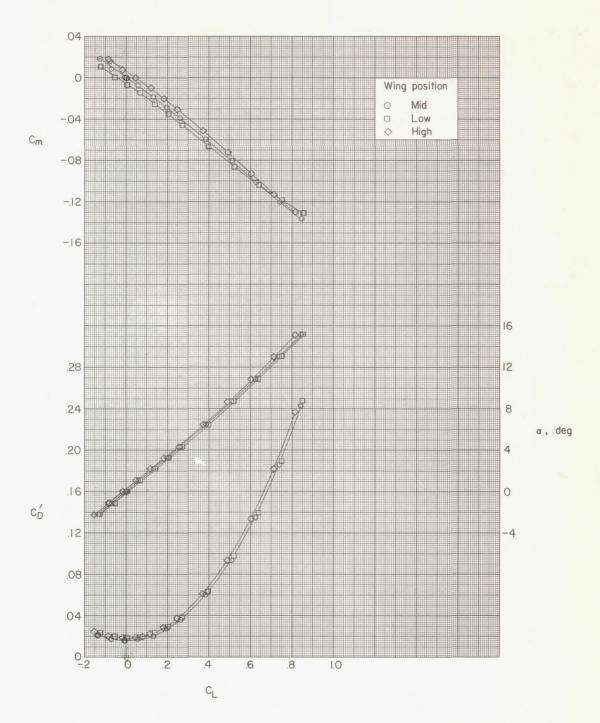
(b) Horizontal tails.

Figure 1.- Concluded.



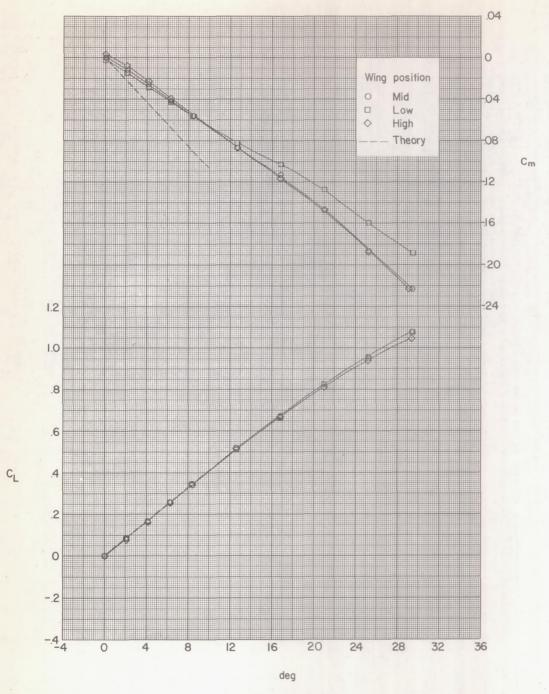
(a) Variation of longitudinal characteristics with angle of attack.

Figure 2.- Effect of wing vertical position on the longitudinal aerodynamic characteristics of the wing-body configuration. M = 1.41.



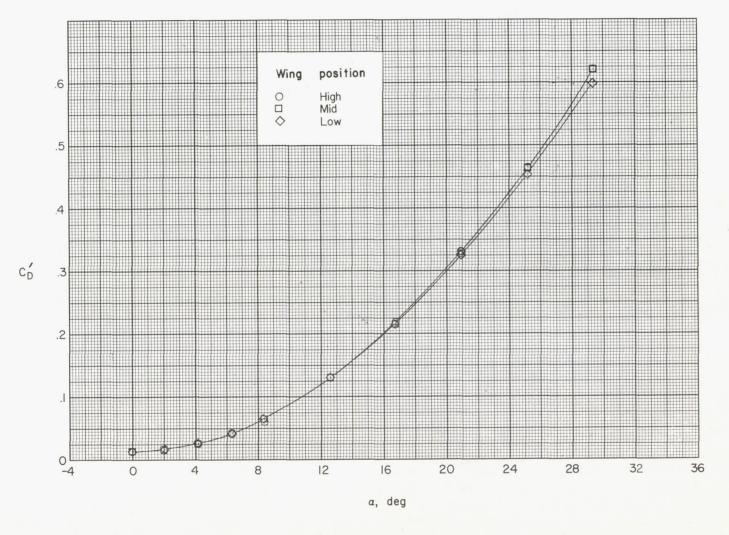
(b) Variation of longitudinal characteristics with lift.

Figure 2.- Concluded.



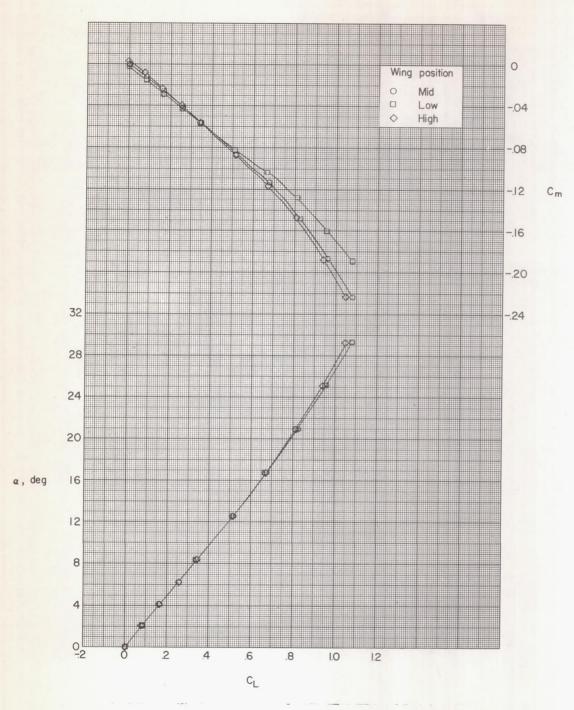
(a) Variation of longitudinal characteristics with angle of attack.

Figure 3.- Effect of wing vertical position on the longitudinal aerodynamic characteristics of the wing-body configuration. M = 2.01.



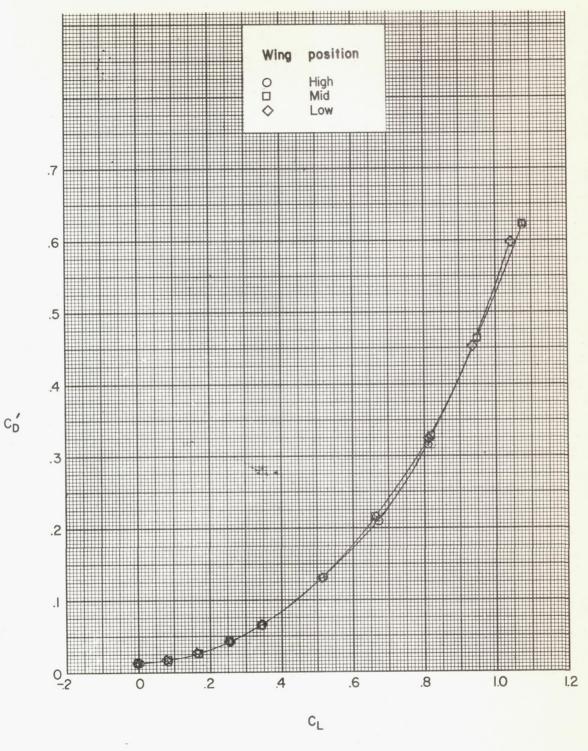
(a) Concluded.

Figure 3. - Continued.



(b) Variation of longitudinal characteristics with lift.

Figure 3.- Continued.



(b) Concluded.

Figure 3.- Concluded.

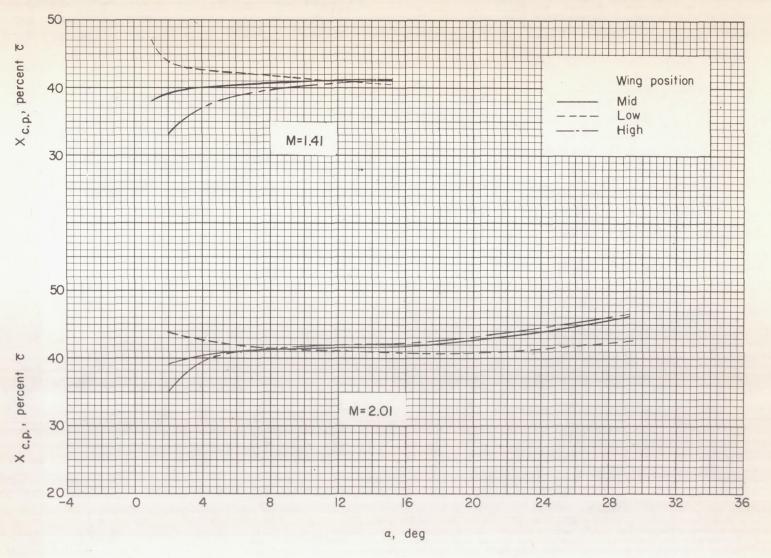


Figure 4.- Effect of wing vertical position on the variation of center of pressure with angle of attack for the wing-body configuration.

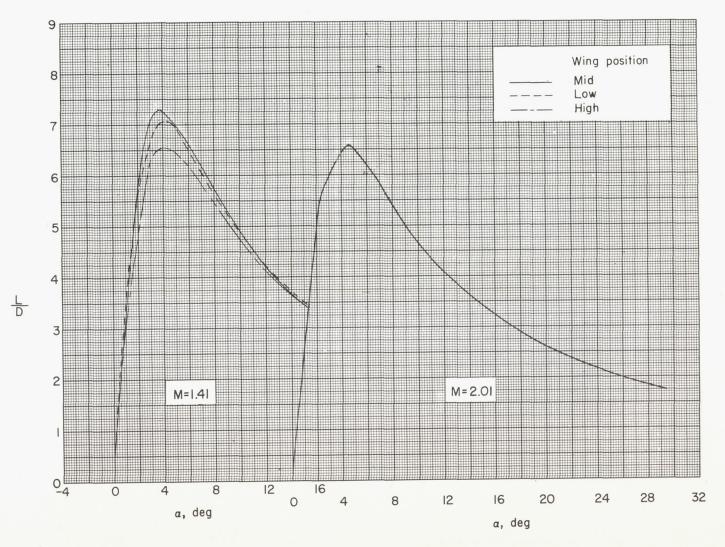


Figure 5.- Effect of wing vertical position on the variation of lift-drag ratio with angle of attack for the wing-body configuration.

.

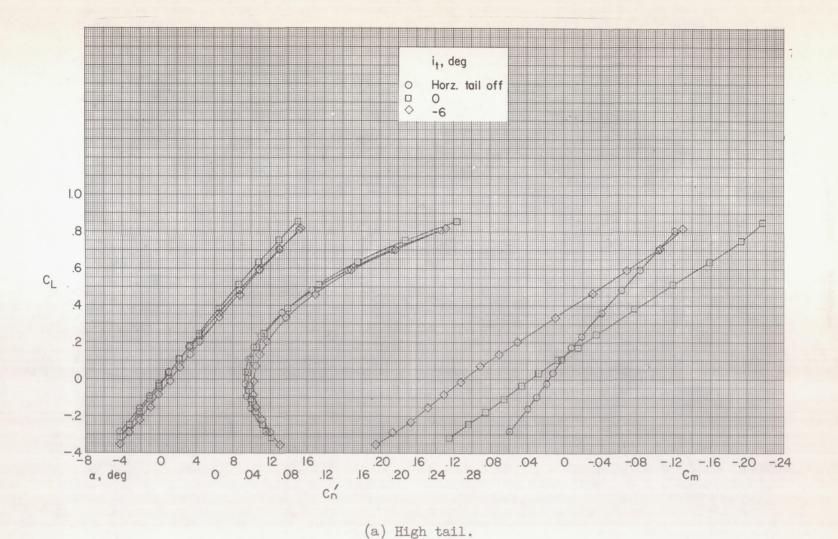
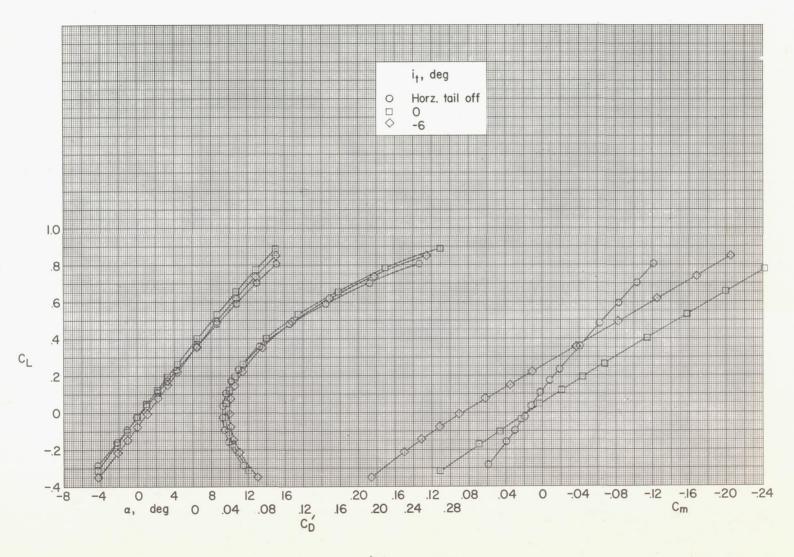


Figure 6.- Longitudinal aerodynamic characteristics of a complete high wing configuration with an unswept horizontal tail. M = 1.41.



(b) Low tail.

Figure 6.- Concluded.

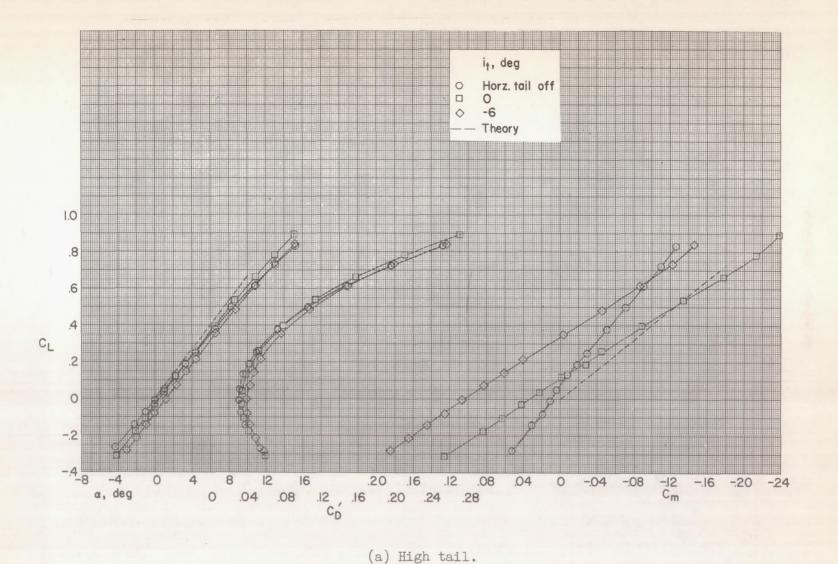
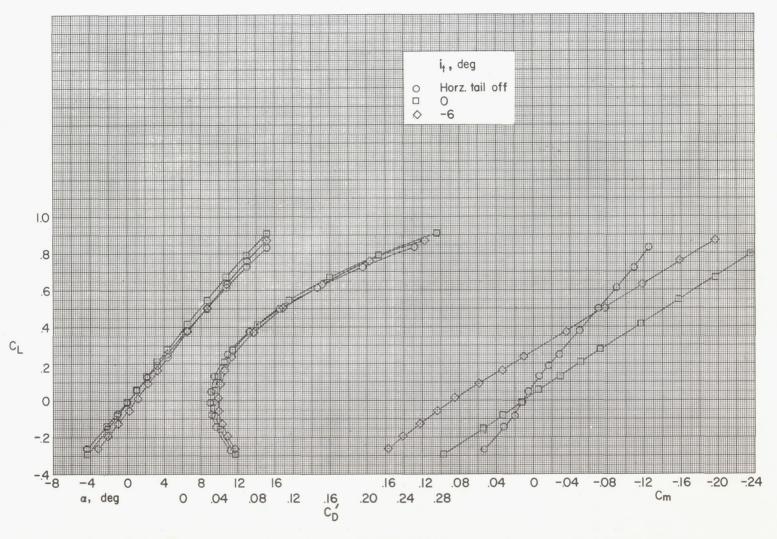


Figure 7.- Longitudinal aerodynamic characteristics of a complete midwing configuration with an unswept horizontal tail. M = 1.41.



(b) Low tail.

Figure 7.- Concluded.

B

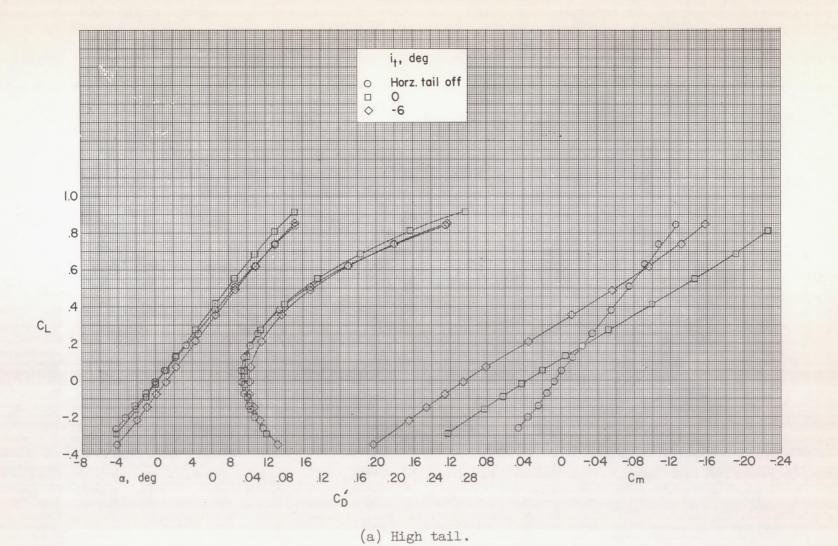
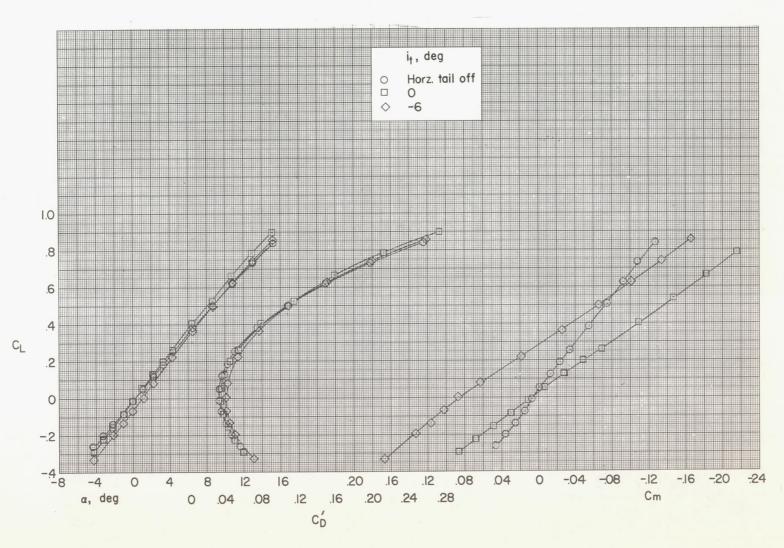


Figure 8.- Longitudinal aerodynamic characteristics of a complete low wing configuration with an unswept horizontal tail. M = 1.41.



(b) Low tail.

Figure 8.- Concluded.

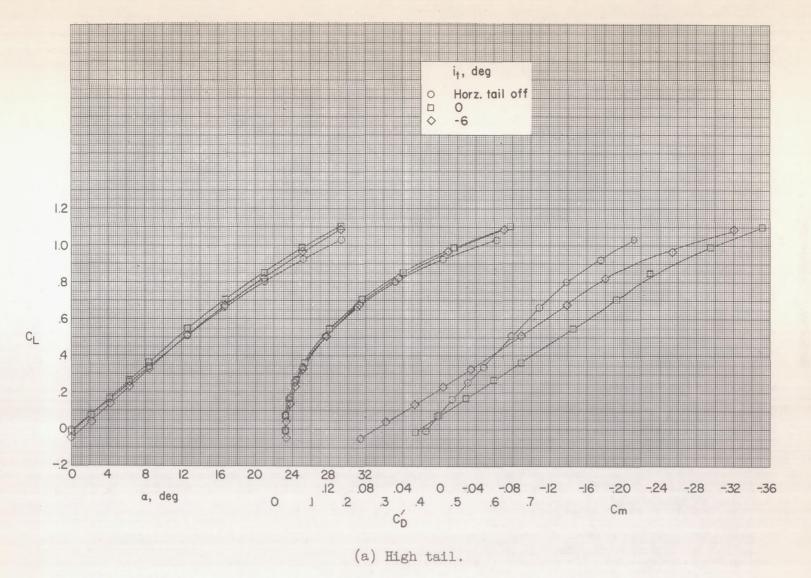
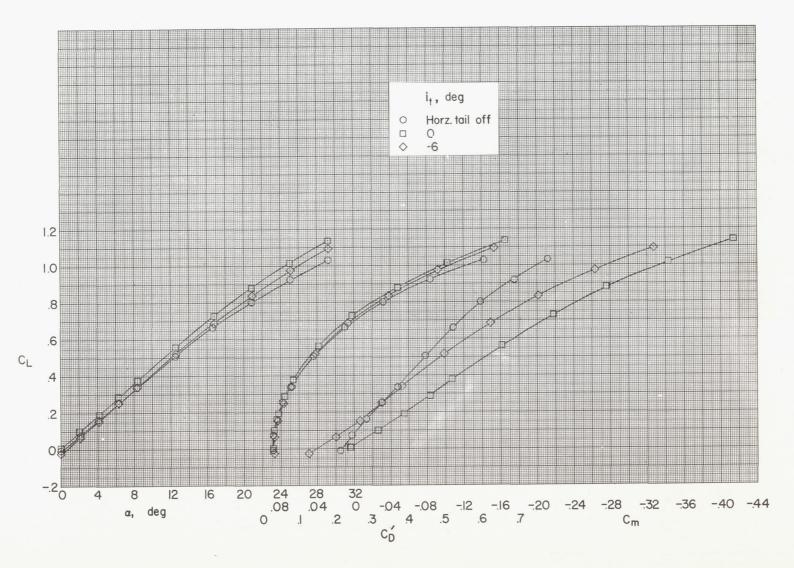


Figure 9.- Longitudinal aerodynamic characteristics of a complete high-wing configuration with an unswept horizontal tail. M = 2.01.



(b) Low tail.

Figure 9.- Concluded.

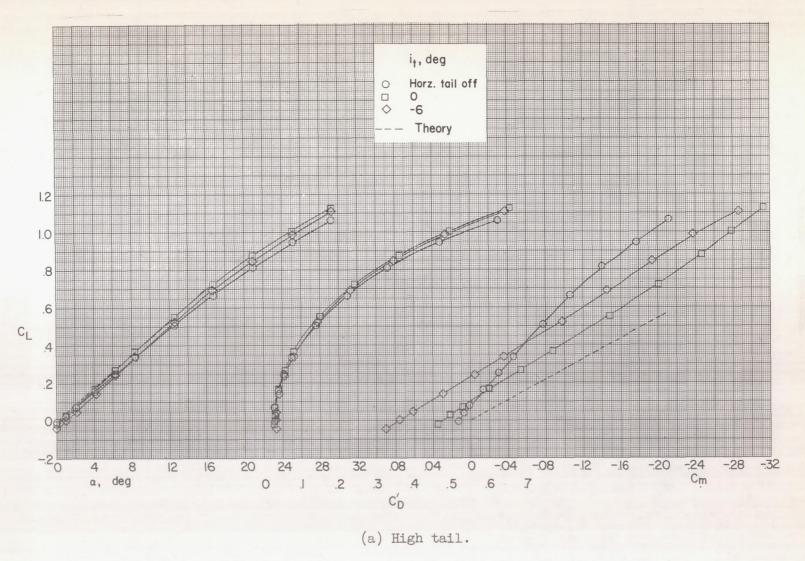
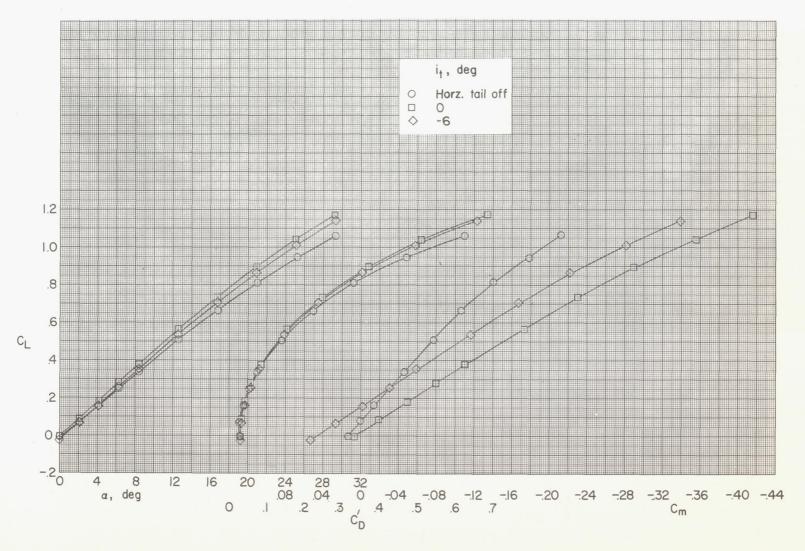


Figure 10.- Longitudinal aerodynamic characteristics of a complete midwing configuration with an unswept horizontal tail. M = 2.01.



(b) Low tail.

Figure 10. - Concluded.

.

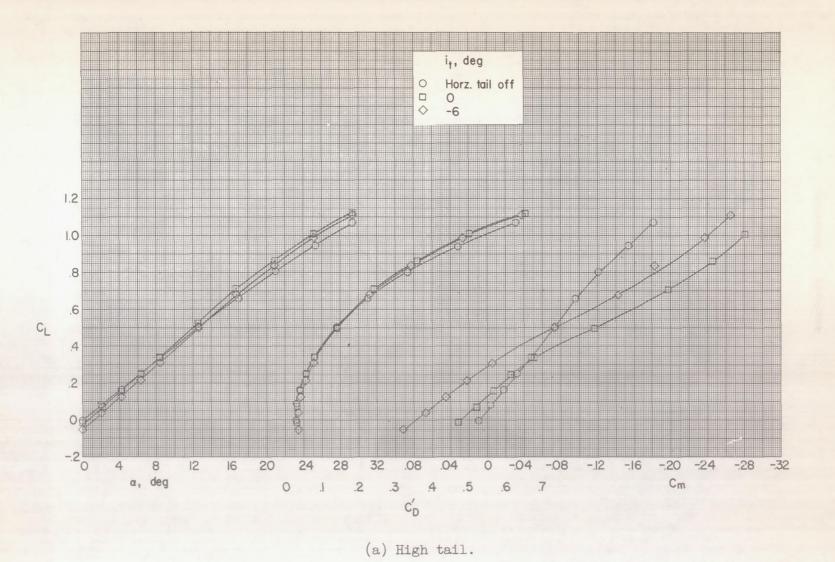
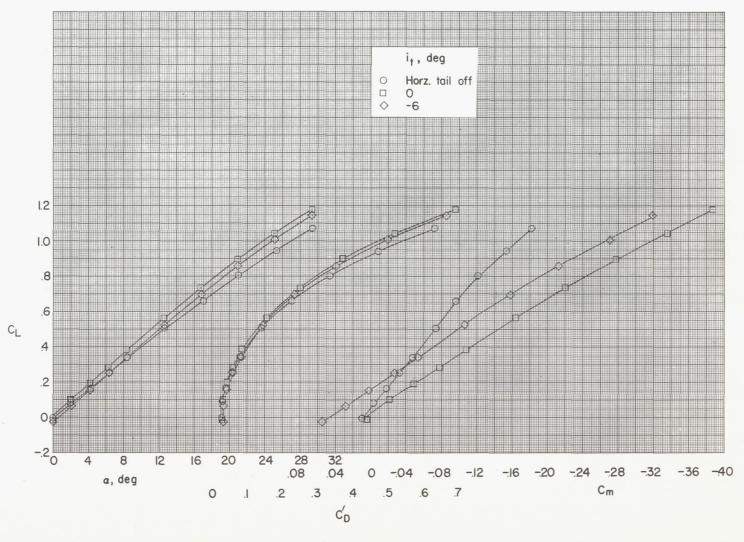


Figure 11.- Longitudinal aerodynamic characteristics of a complete low-wing configuration with an unswept horizontal tail. M = 2.01.



(b) Low tail.

Figure 11. - Concluded.

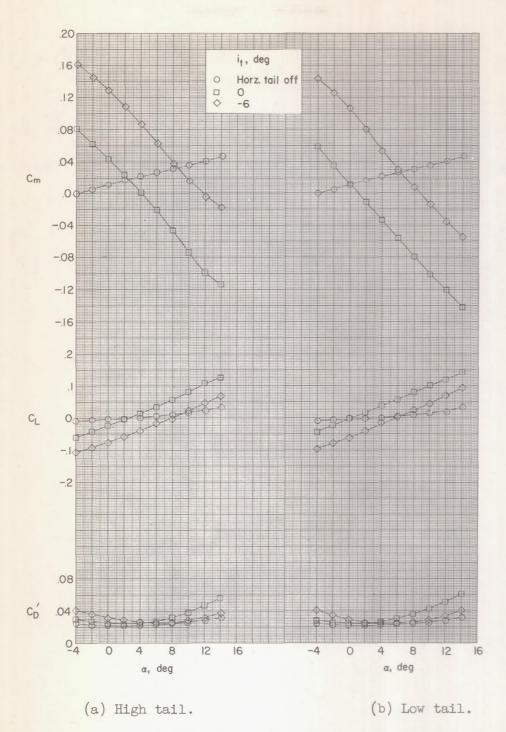
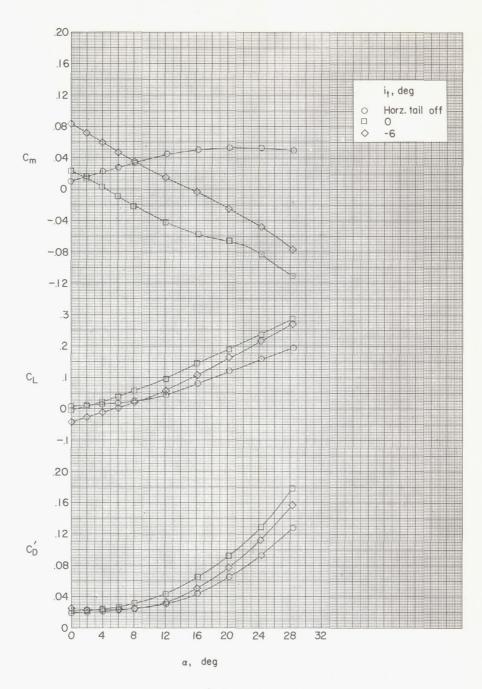
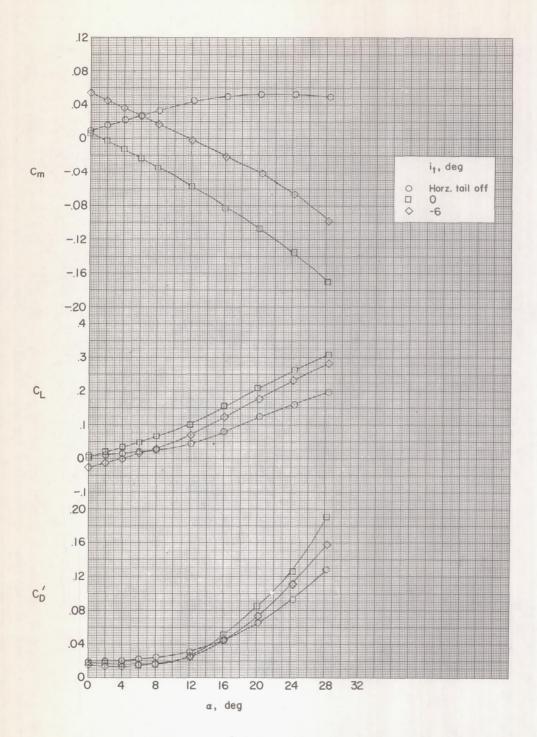


Figure 12.- Longitudinal aerodynamic characteristics of wing-off configuration with the unswept horizontal tail at various vertical positions. M = 1.41.



(a) High tail.

Figure 13.- Longitudinal aerodynamic characteristics of wing-off configuration with the unswept horizontal tail at various vertical positions. M = 2.01.



(b) Low tail.

Figure 13. - Concluded.

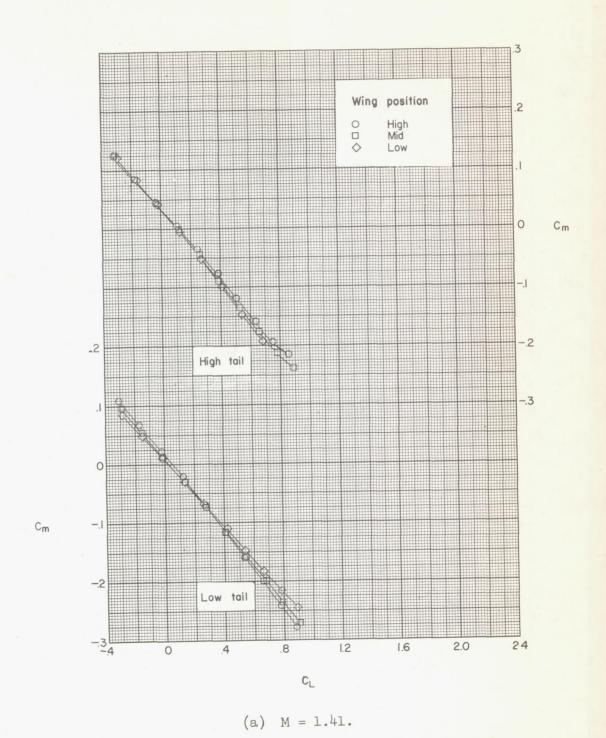
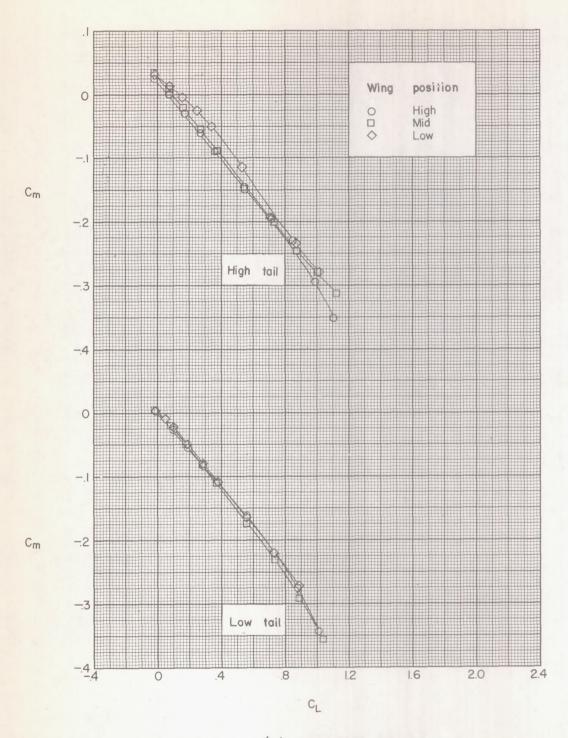


Figure 14. - Effect of wing position on the longitudinal stability characteristics of the complete configurations with various horizontal-tail positions.



(b) M = 2.01.

Figure 14. - Concluded.

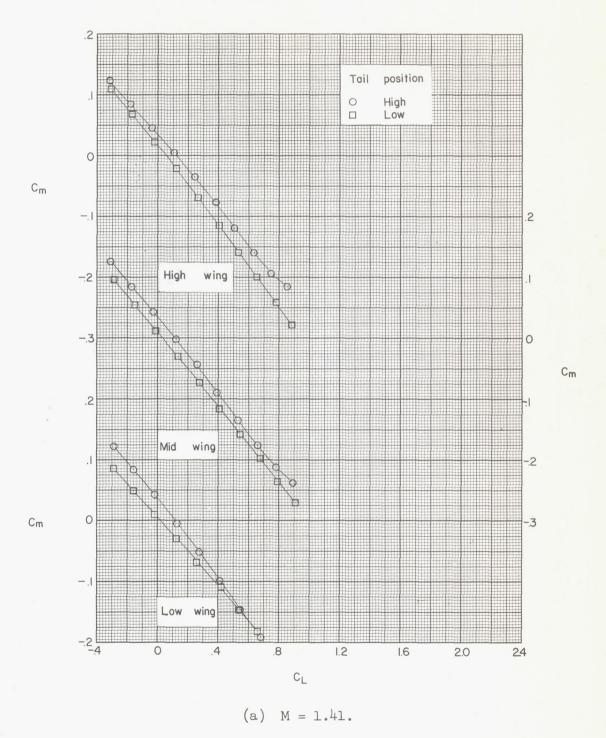


Figure 15.- Effect of horizontal-tail position on the longitudinal stability of the complete configurations with various wing positions.

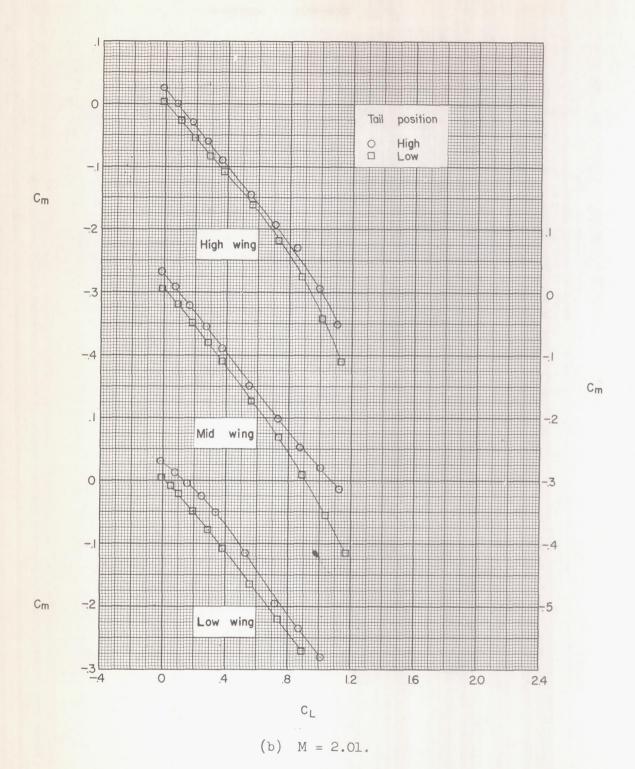


Figure 15. - Concluded.

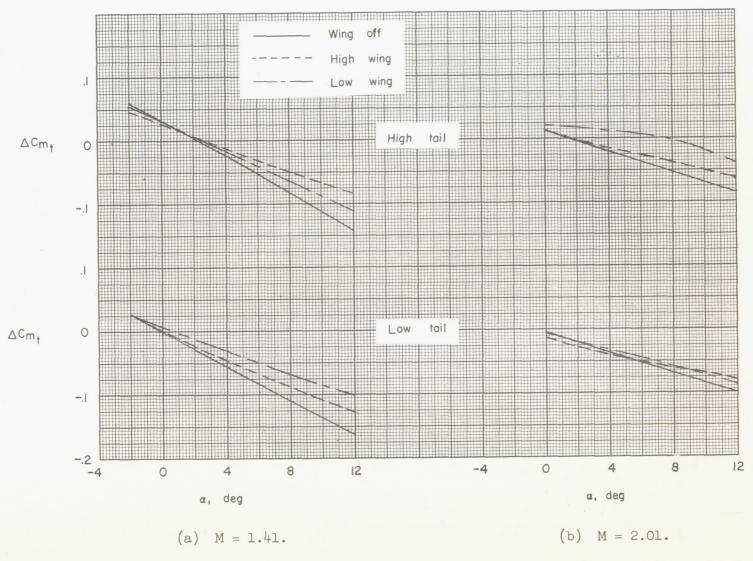
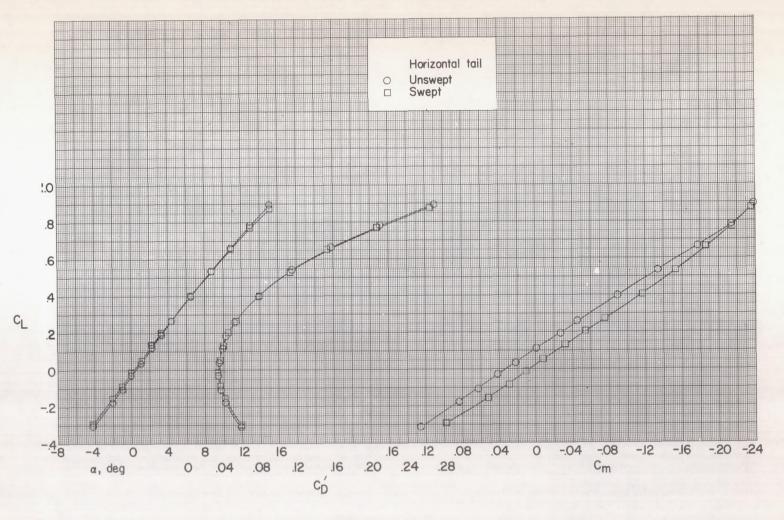


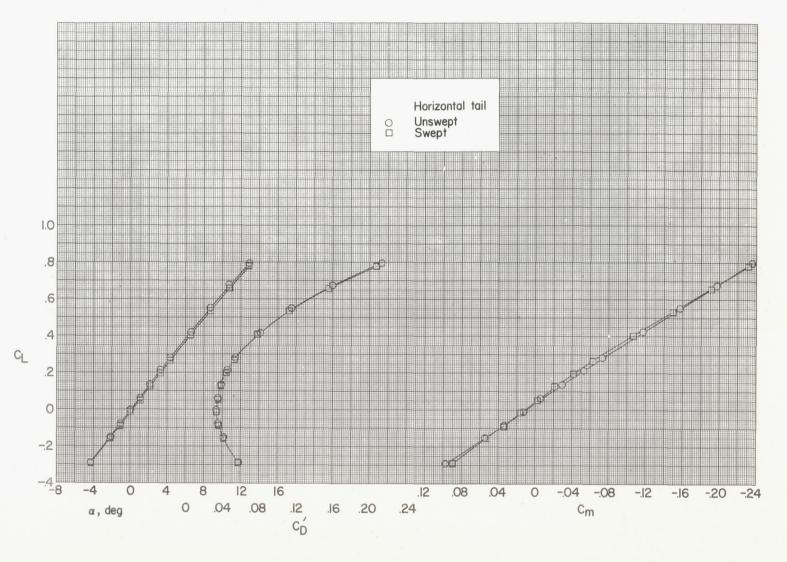
Figure 16.- The effect of wing on the pitching-moment contribution of the unswept horizontal tail.

.



(a) High tail.

Figure 17.- Effect of horizontal tail sweep on the longitudinal aerodynamic characteristics of the complete midwing configuration with the horizontal tail at various vertical positions. M = 1.41.



(b) Low tail.

Figure 17.- Concluded.

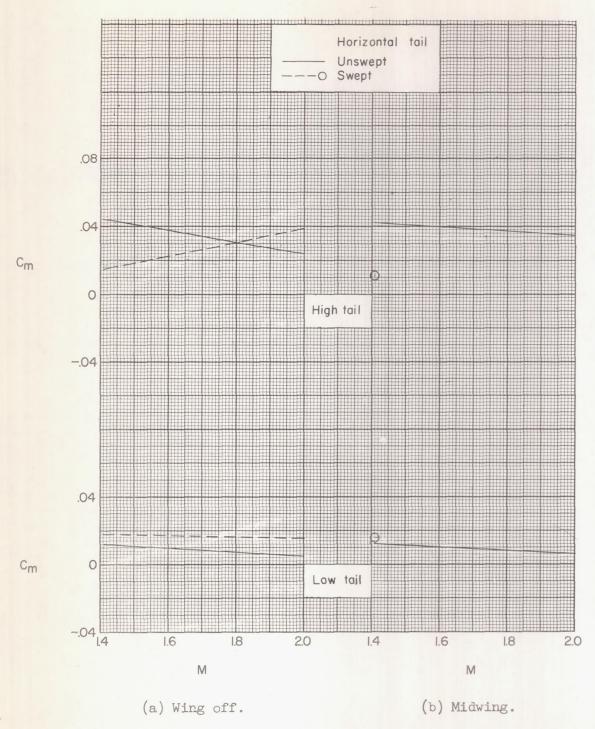


Figure 18.- Effect of horizontal-tail plan form on the pitching-moment coefficients of the wing-off and wing-on configurations at $\alpha = 0^{\circ}$.